

# Additional Goldstone mode and finite temperature effects in strongly phase-separated heteronuclear binary condensates

Arko Roy,<sup>1</sup> S. Gautam,<sup>2</sup> and D. Angom<sup>1</sup>

<sup>1</sup>*Physical Research Laboratory, Navrangpura, Ahmedabad-380009, Gujarat, India*

<sup>2</sup>*Department of Physics, Indian Institute of Science, Bangalore-560012, India*

We examine the Goldstone or zero energy modes of the quasi-1D binary condensate of Rb and Cs at  $T = 0$  as a function of the interspecies interaction. At phase-separation, an additional Goldstone mode appears in the system and persists at higher interspecies interaction for symmetric density profiles. This is not the case for binary condensates with asymmetric profiles. We, then, study evolution of the modes at  $T \neq 0$  using the Hartree-Fock-Bogoliubov theory with Popov approximation. There is mode bifurcation close to the critical temperature, however, the Kohn mode shows deviation from the natural frequency. This is on account of the higher overlap between the thermal and condensate clouds, particularly at the interface in phase-separated domain.

PACS numbers: 03.75.Mn, 03.75.Hh, 67.85.Bc

*Introduction.*— The remarkable feature of two-species Bose-Einstein condensates (TBECs), absent in the single-component BECs, is the phenomenon of phase separation [1, 2]. It occurs when the interspecies interaction potential exceeds the geometric mean of the two intraspecies interaction potential. Experimentally, TBECs have been realized in the mixture of two different alkali atoms [3–5], and in two different isotopes [6] and hyperfine states [7, 8] of an atom. These have led to the theoretical investigations on stationary states [9, 10], dynamical instabilities [11–13] and collective excitations [14–18] of TBECs. At phase separation, the density profiles of a TBEC could be either asymmetric [5, 19, 20] or symmetric [5, 21] depending on the number of atoms and geometry of trapping potential. In experiments, the TBEC can be steered from miscible to phase-separated domain or vice-versa [20, 21] through the interspecies Feshbach resonance. This prompts an interesting question: how do the modes evolve as the TBEC is steered from miscible to phase-separation? A recent work [18] has examined and answered the question for the case of asymmetric density profiles. In this letter we provide an answer to the case of symmetric profiles for a quasi-1D system. One striking result is, the additional Goldstone mode emerging at phase-separation evolves in a very different way.

Another property of importance is the evolution of the modes with temperature, however, such a study requires finite temperature theories. To include finite temperature effects there are different approaches, such as projected Gross-Pitaevskii (GP) equation [22], stochastic GP equation (SGPE) [23] and Zaremba-Nikuni-Griffin (ZNG) formalism [24]. We have, however, chosen Hartree-Fock-Bogoliubov theory with Popov approximation (HFB-Popov) [25] for the present work as one can obtain the excitation modes without additional calculations. It has been used extensively in single species BEC to study finite temperature effects to mode energies [25–28]. In TBECs, the HFB-Popov approximation has been used to study the finite temperature effects in the miscible domain [29] but not in phase-separated domain.

Other works which have examined the finite temperature effects in TBECs use Hartree-Fock treatment with or without trapping potential [30, 31] and semi-classical approach [32]. Although, HFB-Popov does have the advantage vis-a-vis calculation of the modes, it is nontrivial to get converged solutions. In this letter we consider the TBEC of  $^{87}\text{Rb}$ - $^{133}\text{Cs}$  [4, 5], which have widely differing  $s$ -wave scattering lengths and masses. This choice does add to the severity of the convergence issues but this also makes it a good test for the methods we use. Furthermore, in this system the background  $s$ -wave scattering lengths satisfy the condition of phase-separation.

The quasi-1D trapped bosons exhibit a rich phase structure as a function of density and interaction strengths [33]. In this work, as mentioned earlier, we choose the parameter domain where the system is quasi-1D and a mean-field description like HFB-Popov is applicable. However, mean field theories must be used with care in quasi-1D systems as it breaks down at temperatures close to the ground state of the transverse potential [34]. So, in this work we examine the TBEC of  $^{87}\text{Rb}$ - $^{133}\text{Cs}$  at temperatures close to the critical temperature of the longitudinal potential, which is much lower than the transverse one. We also study the system, using quasi-1D description, with the parameters as in the experiment [5]. We find that, like in Ref. [35], the quasi-1D description are in good agreement with the condensate density profiles of 3D calculations [36]. It must be mentioned that, in previous works, SGPE was used to probe the existence of quasi-condensates in quasi-1D systems [37, 38].

*Theory.*— For a highly anisotropic cigar shaped trapping potential ( $\omega_x = \omega_y \gg \omega_z$ ) we can integrate out the condensate wave function along  $xy$  and reduce it to a quasi-1D system. The grand-canonical Hamiltonian, in second quantized form, describing the mixture of two

interacting BECs is then

$$H = \sum_{k=1,2} \int dz \hat{\Psi}_k^\dagger(z,t) \left[ -\frac{\hbar^2}{2m_k} \frac{\partial^2}{\partial z^2} + V_k(z) - \mu_k \right. \\ \left. + \frac{U_{kk}}{2} \hat{\Psi}_k^\dagger(z,t) \hat{\Psi}_k(z,t) \right] \hat{\Psi}_k(z,t) \\ + U_{12} \int dz \hat{\Psi}_1^\dagger(z,t) \hat{\Psi}_2^\dagger(z,t) \hat{\Psi}_1(z,t) \hat{\Psi}_2(z,t), \quad (1)$$

where  $k = 1, 2$  is the species index,  $\hat{\Psi}_k$ 's are the Bose field operators of the two different species, and  $\mu_k$ 's are the chemical potentials. The strength of intra and inter-species repulsive interactions are  $U_{kk} = (a_{kk}\lambda)/m_k$  and  $U_{12} = (a_{12}\lambda)/(2m_{12})$ , respectively, where  $\lambda = (\omega_x/\omega_z) \gg 1$  is the anisotropy parameter,  $a_{kk}$  is the  $s$ -wave scattering length,  $m_k$ 's are the atomic masses of the species and  $m_{12} = m_1 m_2 / (m_1 + m_2)$  and  $\cdot$ . Starting with this Hamiltonian, the equation of motion of the Bose field operators is

$$i\hbar \frac{\partial}{\partial t} \begin{pmatrix} \hat{\Psi}_1 \\ \hat{\Psi}_2 \end{pmatrix} = \begin{pmatrix} \hat{h}_1 + U_{11} \hat{\Psi}_1^\dagger \hat{\Psi}_1 & U_{12} \hat{\Psi}_2^\dagger \hat{\Psi}_1 \\ U_{12} \hat{\Psi}_1^\dagger \hat{\Psi}_2 & \hat{h}_2 + U_{22} \hat{\Psi}_2^\dagger \hat{\Psi}_2 \end{pmatrix} \begin{pmatrix} \hat{\Psi}_1 \\ \hat{\Psi}_2 \end{pmatrix}$$

where  $\hat{h}_k = (-\hbar^2/2m_k)\partial^2/\partial z^2 + V_k(z) - \mu_k$ . For compact notations, we refrain from writing the explicit dependence of  $\hat{\Psi}_k$  on  $z$  and  $t$ . Since a majority of the atoms reside in the ground state for the temperature regime relevant to the experiments ( $T \leq 0.65T_c$ ) [27], the condensate part can be separated out from the Bose field operator  $\hat{\Psi}(\mathbf{r}, t)$ . The non-condensate or the thermal cloud of atoms are then the fluctuations of the condensate field. Here,  $T_c$  is the critical temperature of ideal gas in a harmonic confining potential. Accordingly, we define [25],  $\hat{\Psi}(z, t) = \hat{\Phi}(z) + \tilde{\Psi}(z, t)$ , where  $\hat{\Phi}(z)$  is a  $c$ -field and represents the condensate, and  $\tilde{\Psi}(z, t)$  is the fluctuation part. In two component representation

$$\begin{pmatrix} \hat{\Psi}_1 \\ \hat{\Psi}_2 \end{pmatrix} = \begin{pmatrix} \phi_1 \\ \phi_2 \end{pmatrix} + \begin{pmatrix} \tilde{\psi}_1 \\ \tilde{\psi}_2 \end{pmatrix}, \quad (2)$$

where  $\phi_k(z)$  and  $\tilde{\psi}_k(z)$  are the condensate and fluctuation part of the  $k$ th species. Thus for a TBEC, the equation of motion of the condensate within the time-independent HFB-Popov approximation is given by the coupled generalized GP equations

$$\hat{h}_1 \phi_1 + U_{11} [n_{c1} + 2\tilde{n}_1] \phi_1 + U_{12} n_2 \phi_1 = 0, \quad (3a)$$

$$\hat{h}_2 \phi_2 + U_{22} [n_{c2} + 2\tilde{n}_2] \phi_2 + U_{12} n_1 \phi_2 = 0. \quad (3b)$$

In the above equation,  $n_{ck}(z) \equiv |\phi_k(z)|^2$ ,  $\tilde{n}_k(z) \equiv \langle \tilde{\psi}_k^\dagger(z, t) \tilde{\psi}_k(z, t) \rangle$ , and  $n_k(z) = n_{ck}(z) + \tilde{n}_k(z)$  are the local condensate, non-condensate, and total density, respectively. Using Bogoliubov transformation, the fluctuations are

$$\tilde{\psi}_k(z, t) = \sum_j \left[ u_{kj}(z) \hat{\alpha}_j(z) e^{-iE_j t} - v_{kj}^*(z) \hat{\alpha}_j^\dagger(z) e^{iE_j t} \right], \\ \tilde{\psi}_k^\dagger(z, t) = \sum_j \left[ u_{kj}^*(z) \hat{\alpha}_j^\dagger(z) e^{iE_j t} - v_{kj}(z) \hat{\alpha}_j(z) e^{-iE_j t} \right].$$

Here,  $\hat{\alpha}_j$  ( $\hat{\alpha}_j^\dagger$ ) are the quasiparticle annihilation (creation) operators and satisfy the usual Bose commutation relations, and the subscript  $j$  represents the energy eigenvalue index. We define the operators as common to both the species, which is natural and consistent as the dynamics of the species are coupled. Furthermore, this reproduces the standard coupled Bogoliubov-de Gennes equations at  $T = 0$  [18] and in the limit  $a_{12} \rightarrow 0$ , non-interacting TBEC, the quasi-particle spectra separates into two distinct sets: one set for each of the condensates. From the above definitions, we get the following Bogoliubov-de Gennes equations

$$\hat{\mathcal{L}}_1 u_{1j} - U_{11} \phi_1^2 v_{1j} + U_{12} \phi_1 (\phi_2^* u_{2j} - \phi_2 v_{2j}) = E_j u_{1j}, \quad (4a)$$

$$\hat{\mathcal{L}}_1 v_{1j} + U_{11} \phi_1^* u_{1j} - U_{12} \phi_1^* (\phi_2 v_{2j} - \phi_2^* u_{2j}) = E_j v_{1j}, \quad (4b)$$

$$\hat{\mathcal{L}}_2 u_{2j} - U_{22} \phi_2^2 v_{2j} + U_{12} \phi_2 (\phi_1^* u_{1j} - \phi_1 v_{1j}) = E_j u_{2j}, \quad (4c)$$

$$\hat{\mathcal{L}}_2 v_{2j} + U_{22} \phi_2^* u_{2j} - U_{12} \phi_2^* (\phi_1 v_{1j} - \phi_1^* u_{1j}) = E_j v_{2j}, \quad (4d)$$

where  $\hat{\mathcal{L}}_1 = (\hat{h}_1 + 2U_{11}n_1 + U_{12}n_2)$ ,  $\hat{\mathcal{L}}_2 = (\hat{h}_2 + 2U_{22}n_2 + U_{12}n_1)$  and  $\hat{\mathcal{L}}_k = -\hat{\mathcal{L}}_k$ . To solve Eq. (4) we define  $u_k$  and  $v_k$ 's as linear combination of the harmonic oscillator eigenstates. The equation is then reduced to a matrix eigenvalue equation and solved using standard matrix diagonalization algorithms. The number density  $\tilde{n}_k$  of non-condensate particles is then

$$\tilde{n}_k = \sum_j \{ |u_{kj}|^2 + |v_{kj}|^2 \} N_0(E_j) + |v_{kj}|^2 \quad (5)$$

where  $\langle \hat{\alpha}_j^\dagger \hat{\alpha}_j \rangle = (e^{\beta E_j} - 1)^{-1} \equiv N_0(E_j)$  is the Bose factor of the quasi-particle state with energy  $E_j$ . The coupled Eqns. (3),(4) are solved iteratively till the desired accuracy is reached. During the iteration, to avoid metastable states, we impose the condition that  $E_j$ 's are real.

*Zero temperature results.*— In binary condensates, phase separation occurs when  $U_{12} > \sqrt{U_{11}U_{22}}$ . For the present work on the  $^{87}\text{Rb}$ - $^{133}\text{Cs}$  mixture, we consider Cs and Rb as the first and second species, respectively. With this identification  $a_{11} = 280a_0$  and  $a_{22} = 100a_0$  are  $a_{\text{CsCs}}$  and  $a_{\text{RbRb}}$ , respectively. Similarly,  $a_{12}$  is  $a_{\text{CsRb}}$  and arrive at the condition for phase separation as  $a_{\text{CsRb}} > 261a_0$ , which is smaller than the background value of  $a_{\text{CsRb}} \approx 650a_0$  [4]. To examine the nature of the modes in the neighbourhood of phase separation, we compute the excitation spectrum at  $T = 0$  and vary  $a_{\text{CsRb}}$ . This maybe possible using the Rb-Cs Feshbach resonance [39] in the  $^{87}\text{Rb}$ - $^{133}\text{Cs}$  experiments with optical traps [4, 5]. The evolution of the low-lying modes in the domain  $0 \leq a_{\text{CsRb}} \leq 450a_0$  with  $N_{\text{Rb}} = N_{\text{Cs}} = 10^4$  are computed with  $\omega_z(\text{Rb}) = 2\pi \times 3.89\text{Hz}$  and  $\omega_z(\text{Cs}) = 2\pi \times 4.55\text{Hz}$  as in ref. [5, 36]. However, to form a quasi-1D system we take  $\omega_\perp = 50\omega_z$ , so that  $\hbar\omega_\perp \gg \mu_k$ . For these values, the relevant quasi-1D parameters  $\alpha = 2a_{\text{CsCs}} \sqrt{(\omega_\perp/\omega_z)(m\omega_\perp/\hbar)} \approx 0.36$  and  $\gamma = 2(a_{\text{CsCs}}/n_{\text{Cs}})(m\omega_\perp/\hbar) \approx 10^{-5}$ , so the system is in the weakly interacting TF regime [33] and mean field description through GP-equation is valid. For this set of

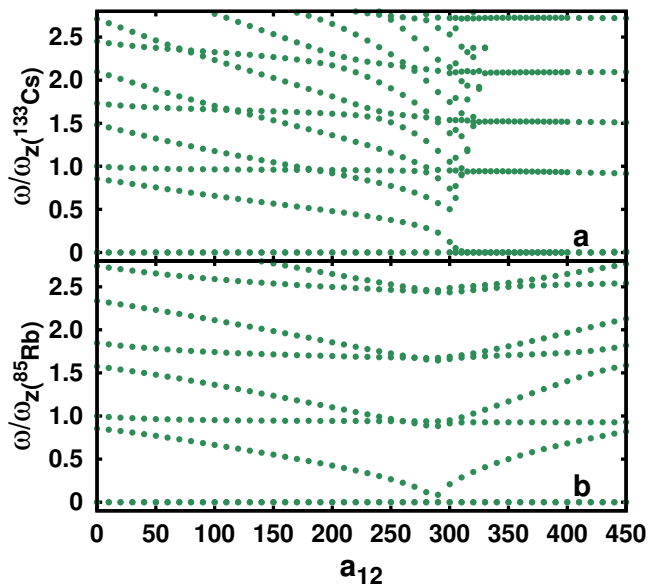


FIG. 1. Evolution of the low-lying modes of the binary condensate as a function of the inter-species scattering length  $a_{12}$ . (a) Low-lying modes of  $^{87}\text{Rb}$ - $^{133}\text{Cs}$  binary condensate for  $N_{87\text{Rb}} = N_{133\text{Cs}} = 10^4$ . At phase separation, the density profiles of the condensates are symmetric and some of the modes disappear as these are energetically unfavourable. (b) Low-lying modes of  $^{85}\text{Rb}$ - $^{87}\text{Rb}$  for  $N_{87\text{Rb}} = N_{85\text{Cs}} = 10^2$ . At phase separation the density profiles are asymmetric and one of the modes goes soft.

parameters the ground state of the TBEC is symmetric and we consider same  $\omega_z$  in the other calculations as well. In the computations we scale the spatial and temporal variables as  $z/a_{\text{osc}(\text{Cs})}$  and  $\omega_{z(\text{Cs})}t$  which render the equations dimensionless. At  $T = 0$ ,  $N_0(E_j)$ 's in Eq. (5) are zero and solving the equations is a one time diagonalization of Eq. (4) as self-consistency is not required. When  $a_{\text{CsRb}} = 0$ , the  $U_{\text{CsRb}}$  dependent terms in Eq.(4) are zero and the spectrum of the two species are independent as the two condensates are decoupled. The system has two Goldstone modes, one each for the two species. The two lowest modes with nonzero excitation energies are the Kohn modes of the two species, and these occur at  $\hbar\omega_{z(\text{Cs})}$  and  $0.85\hbar\omega_{z(\text{Cs})}$  for Cs and Rb species, respectively.

The clear separation between the modes of the two species is lost when  $a_{\text{CsRb}} > 0$  and mixing of modes occurs. For example, the Kohn modes of the two species intermix when  $a_{\text{CsRb}} > 0$ , however, there is a difference in the evolution of the mode energies. The energy of the Rb Kohn mode decreases, but the one corresponding to Cs remains steady at  $\hbar\omega_{z(\text{Cs})}$ . At higher  $a_{\text{CsRb}}$  the energy of the Rb Kohn mode decreases further and goes soft at phase separation ( $U_{\text{CsRb}} > \sqrt{U_{\text{CsCs}}U_{\text{RbRb}}}$ ) when  $a_{\text{CsRb}} \approx 310a_0$ . This introduces a new Goldstone mode of the Rb BEC to the excitation spectrum. The reason is, for the parameters chosen, the density profiles at phase separation are symmetric with Cs BEC at the center and

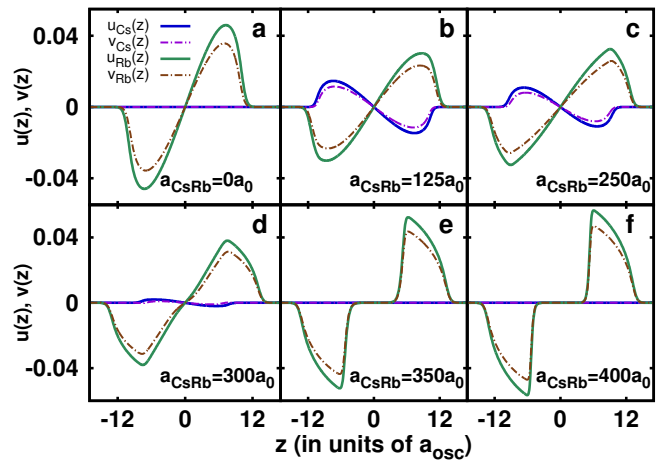


FIG. 2. Evolution of the Rb Kohn mode as  $a_{\text{CsRb}}$  is increased from 0 to  $400a_0$ . For better visibility  $u_{\text{Cs}}$  and  $u_{\text{Rb}}$  are scaled by a factor of 1.2. (a) When  $a_{\text{CsRb}} = 0$ , it is a Kohn mode of the Rb condensate. (b-d) In the domain  $0 < a_{\text{CsRb}} \lesssim 310a_0$  the mode acquires admixtures from the Cs Kohn mode (nonzero  $u_{\text{Cs}}$  and  $v_{\text{Cs}}$ ). (e-f) At phase separation  $310a_0 \lesssim a_{\text{CsRb}}$  the mode transforms to a Goldstone mode:  $u_{\text{Rb}}$  and  $v_{\text{Rb}}$  have same profile as the  $n_{\text{Rb}}$  ( Rb condensate density profile) but with a phase difference.

Rb BEC at the edges. So, the Rb BECs at the edges are effectively two topologically distinct BECs and there are two Goldstone modes with the same  $|u_{\text{Rb}}|$  and  $|v_{\text{Rb}}|$  but different phases.

To examine the mode evolution with the experimentally realized parameters [5], we repeat the computations with  $\omega_{\perp(\text{Cs})} = 2\pi \times 40.2\text{Hz}$  and  $\omega_{\perp(\text{Rb})} = 2\pi \times 32.2\text{Hz}$ . With these parameters the system is not strictly quasi-1D as  $\hbar\omega_{\perp k} \approx \mu_k$  for  $N_{\text{Cs}} = N_{\text{Rb}} = 10^4$ , however, as  $\omega_{zk} \ll \omega_{\perp k}$  there must be qualitative similarities to a quasi-1D system. In this case too, with the variation of  $a_{\text{CsRb}}$  the modes evolve similar to the case of  $\omega_{\perp k} = 50\omega_{zk}$  and energies of the low-lying modes are shown in Fig. 1(a). The evolution of the Rb Kohn mode functions ( $u$  and  $v$ ) with  $a_{\text{CsRb}}$  are shown in Fig. 2. It is evident that when  $a_{\text{CsRb}} = 0$  (Fig. 2(a)), there is no admixture from the Cs Kohn mode ( $u_{\text{Cs}} = v_{\text{Cs}} = 0$ ). However, when  $0 < a_{\text{CsRb}} \lesssim 310a_0$  the admixture from the Cs Kohn mode increases initially and then goes to zero as we approach  $U_{\text{CsRb}} > \sqrt{U_{\text{CsCs}}U_{\text{RbRb}}}$  (Fig. 2(b-f) ).

One striking result is, the Rb Kohn mode after going soft at  $a_{\text{CsRb}} \approx 310a_0$ , as shown in Fig. 1(a), continues as the third Goldstone mode for  $310a_0 < a_{\text{CsRb}}$ . This is very different from the evolution pattern of the soft mode in binary condensates where the density profiles are asymmetric at phase separation. In which case after phase separation, the soft mode regain energy and only two Goldstone modes remain in the system. This is evident from Fig. 1(b), where we show the mode evolution of  $^{85}\text{Rb}$ - $^{87}\text{Rb}$  mixture with asymmetric density profiles at phase separation. The parameters of the system considered are  $N_{85\text{Rb}} = N_{87\text{Rb}} = 10^2$  with the same  $\omega_{zk}$  and

$\omega_{\perp k}$  as in the Rb-Cs mixture. Here, we use intraspecies scattering lengths as  $99a_0$  and  $100a_0$  for  $^{85}\text{Rb}$  and  $^{87}\text{Rb}$ , respectively and tune the interspecies interaction for better comparison with the Rb-Cs results. This is, however, different from the experimental realization [20], where the intra-species interaction of  $^{85}\text{Rb}$  is tuned to avoid the attractive background scattering length as well as examine different phases. But, the nature of the mode evolution is similar to tuning interspecies interaction. A similar result was reported in an earlier work on quasi-2D system of binary condensates [18]. Another remarkable result unique to symmetric density profile at phase separation is, some of the higher energy modes cease to exist around specific values of  $a_{\text{CsRb}}$ . The reason is, modes with interaction energy

$$\Delta E_j = U_{\text{CsRb}} \int |\phi_{\text{Cs}}(z)|^2 |u_{\text{Rb}j}(z) - v_{\text{Rb}j}^*(z)|^2 dz,$$

close to  $E_j = \hbar\omega_j$  are unviable when  $a_{\text{CsRb}}$  is increased further as the Rb condensate atoms require more energy than possible to have non-zero density within the Cs condensate.

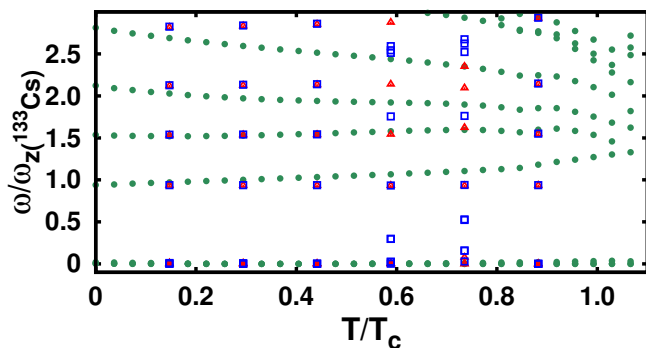


FIG. 3. The excitation energies of the low-lying modes at  $T/T_c \neq 0$ . The filled circles (green) are the excitation energies from the HFB-Popov theory with  $N_{\text{Rb}} = N_{\text{Cs}} = 10^3$ . The squares (blue) are the excitation energies at  $T/T_c = 0$ , but with the number of condensate atoms ( $N_{c(\text{Rb})}$  and  $N_{c(\text{Cs})}$ ) equal to the  $T/T_c \neq 0$  case. The triangles (red) are results from computations with the same  $N_{c(\text{Rb})}$  and  $N_{c(\text{Cs})}$ , but at  $T/T_c = 10^{-20}\text{K}$ .

*Finite temperature results.*— For the  $T \neq 0$  calculations, as mentioned earlier, we solve the coupled Eq. (3) and (4) iteratively till convergence. After each iteration,  $\phi_k(z)$  are renormalized so that

$$\int_{-\infty}^{\infty} [|\phi_k(z)|^2 + \tilde{n}_k(z)] dz = N_k, \quad (6)$$

where  $k$  is either Rb or Cs. To improve convergence, we use successive over relaxation, but at higher  $T$  we face difficulties and require careful choice of the relaxation parameters. For computations, we again consider the trap parameters  $\omega_{\perp(\text{Cs})} = 2\pi \times 40.2\text{Hz}$  and  $\omega_{\perp(\text{Rb})} = 2\pi \times 32.2\text{Hz}$  with coinciding trap centers, the number of

atoms as  $N_{\text{Rb}} = N_{\text{Cs}} = 10^3$  and  $a_{\text{CsRb}} = 650a_0$ . The evolution of  $\omega$  (mode frequency) with  $T$  is shown in Fig. 3, where the  $T$  is in units of  $T_c$ , the critical temperature of ideal bosons in quasi-1D harmonic traps defined through the relation  $N = (k_{\text{B}}T_c/\hbar\omega_z) \ln(2k_{\text{B}}T_c/\hbar\omega_z)$  [40]. From the figure, when  $T/T_c \geq 0.2$  the Kohn mode energy increases with  $T/T_c$ . This is consistent with an earlier work on HFB-Popov studies in single species condensate [28]. It is, however, different from the trend observed in ref. [26, 27]. This indicates the short comings of excluding  $\tilde{n}$  from the dynamics in HFB-Popov theory. In binary condensates, however, the deviations from neglecting  $\tilde{n}$  in the dynamics may be larger as  $\tilde{n}$  is large at the interface. The Goldstone modes, not surprisingly, remain steady at  $\omega = 0$  for all  $T/T_c$ .

The trend in the evolution of the modes indicates bifurcations at  $T/T_c \approx 1$  and is consistent with the theoretical observations in single species condensates [26–28]. In the case of single species calculations, at  $T/T_c > 1$  the mode frequencies coalesce to the mode frequencies of the trapping potential. In the present work, we, however, limit the calculations to  $0 \leq T/T_c \leq 1.1$ . The results for  $T/T_c > 0.65$  may have significant errors as the HFB-Popov theory gives accurate results at  $T/T_c \leq 0.65$  [27]. We have, however, extended the calculations to  $T/T_c > 0.65$  like in Ref. [26] to study the mode bifurcation.

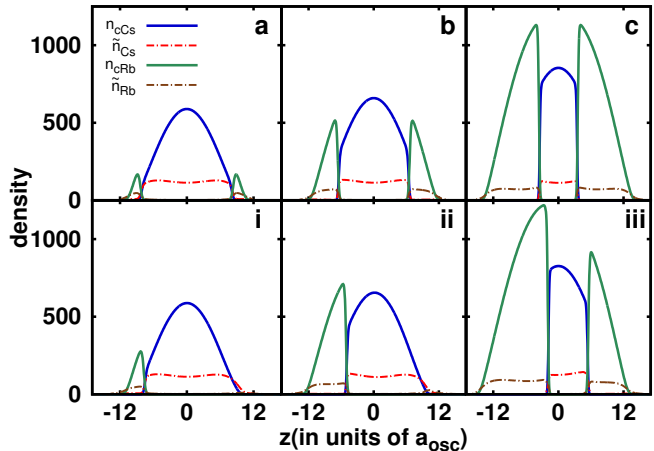


FIG. 4. Density profile of  $n_c$  and  $\tilde{n}$  at 25nK. (a), (b) and (c) correspond to  $N_{\text{Rb}} = 840(N_{\text{Cs}} = 8570)$ ,  $N_{\text{Rb}} = 3680(N_{\text{Cs}} = 8510)$ , and  $N_{\text{Rb}} = 15100(N_{\text{Cs}} = 6470)$ , respectively, with coincident trap centers. (i), (ii) and (iii) correspond to same atom numbers as the previous sequence, however, the trap centers are shifted relatively by  $0.8a_{\text{osc}(\text{Cs})}$ .

To examine the profiles of  $n_{ck}$  and  $\tilde{n}_k$ , we compute the densities at 25nK for three cases, these are  $N_{\text{Rb}} = 840(N_{\text{Cs}} = 8570)$ ,  $N_{\text{Rb}} = 3680(N_{\text{Cs}} = 8510)$ , and  $N_{\text{Rb}} = 15100(N_{\text{Cs}} = 6470)$ . The same set was used in the previous work of Pattinson, et al. at  $T = 0$  [36] and corresponds to three regimes considered ( $N_{\text{Cs}} > N_{\text{Rb}}$ ,  $N_{\text{Cs}} \approx N_{\text{Rb}}$ , and  $N_{\text{Cs}} < N_{\text{Rb}}$ ) in the experimental work of McCarron, et al. [5]. Consider the trap centers, along

$z$ -axis, are coincident, then  $\tilde{n}_k$  and  $n_{ck}$  are symmetric about  $z = 0$ , and are shown in Fig. 4(a-c). In all the cases, with different numbers of atoms, the Cs condensate is at the center. This configuration energetically preferred as heavier atomic species at the center has smaller trapping potential energy and lowers the total energy. In the experiments, the trap centers are not exactly coincident. So, to replicate the experimental situation we shift the trap centers, along  $z$ -axis, by  $0.8a_{\text{osc}(\text{Cs})}$ . The density profiles for three choice of the atomic numbers, shown in Fig. 4(i-iii), are asymmetric. More importantly, for  $N_{\text{Rb}} = 840(N_{\text{Cs}} = 8570)$  and  $N_{\text{Rb}} = 3680(N_{\text{Cs}} = 8510)$  the  $n_{ck}$  and  $\tilde{n}_k$  are located sideways. So, there are only two Goldstone modes in the excitation spectrum. But, for  $N_{\text{Rb}} = 15100(N_{\text{Cs}} = 6470)$ , the Cs condensate is at the center with Rb condensates at the edges and has three Goldstone modes. In all the cases  $\tilde{n}_k$  have maxima in the neighbourhood of the interface and the respective  $n_{ck}$ s are not negligible. So, we can expect larger  $n_{ck}$ - $\tilde{n}_k$  coupling in binary condensates than single species

condensates. For the  $N_{\text{Rb}} = 3680(N_{\text{Cs}} = 8510)$  and  $N_{\text{Rb}} = 15100(N_{\text{Cs}} = 6470)$  cases,  $n_{ck}$  are very similar to the results of 3D calculations at  $T = 0$  [36]. However, it requires a 3D calculation to reproduce  $n_{ck}$  for  $N_{\text{Rb}} = 840(N_{\text{Cs}} = 8570)$  as the relative shift  $\delta x$  is crucial in this case.

*Conclusion.*—In binary condensates a third Goldstone mode emerges in the strongly phase-separated domain. The mode continues to higher interspecies interactions when the condensate density profiles are symmetric. At higher interspecies interactions, some of the modes are unviable, these cease to exist and coalesce with nearby modes. At finite temperatures,  $\tilde{n}_k$  is large at the interface and the  $n_{ck}$ - $\tilde{n}_k$  coupling could be large. This could contribute to deviations of the results from the experimental data.

*Acknowledgement.*—We thank K. Suthar and S. Chattopadhyay for useful discussions. The results presented in the paper are based on the computations using the 3TFLOP HPC Cluster at Physical Research Laboratory, Ahmedabad, India.

- 
- [1] T.-L. Ho and V. B. Shenoy, Phys. Rev. Lett. **77**, 3276 (1996).
- [2] M. Trippenbach *et al.*, J. Phys. B **33**, 4017 (2000).
- [3] G. Modugno *et al.* Phys. Rev. Lett. **89**, 190404 (2002).
- [4] A. Lercher *et al.* Euro. Phys. Jour. D **65**, 3 (2011).
- [5] D. J. McCarron *et al.*, Phys. Rev. A **84**, 011603 (2011).
- [6] S. Inouye *et al.*, Nature **392**, 151 (1998).
- [7] D. M. Stamper-Kurn *et al.*, Phys. Rev. Lett. **80**, 2027 (1998).
- [8] C. J. Myatt *et al.*, Phys. Rev. Lett. **78**, 586 (1997).
- [9] S. Gautam and D. Angom, J. Phys. B **43**, 095302 (2010).
- [10] S. Gautam and D. Angom, J. Phys. B **44**, 025302 (2011).
- [11] K. Sasaki, N. Suzuki, D. Akamatsu, and H. Saito, Phys. Rev. A **80**, 063611 (2009).
- [12] S. Gautam and D. Angom, Phys. Rev. A **81**, 053616 (2010).
- [13] T. Kadokura *et al.*, Phys. Rev. A **85**, 013602 (2012).
- [14] S. Stringari, Phys. Rev. Lett. **77**, 2360 (1996).
- [15] H. Pu and N. P. Bigelow, Phys. Rev. Lett. **80**, 1134 (1998).
- [16] R. Graham and D. Walls, Phys. Rev. A **57**, 484 (1998).
- [17] D. Gordon and C. M. Savage, Phys. Rev. A **58**, 1440 (1998).
- [18] C. Ticknor, Phys. Rev. A **88**, 013623 (2013).
- [19] D. S. Hall *et al.*, Phys. Rev. Lett. **81**, 1539 (1998).
- [20] S. B. Papp, J. M. Pino, and C. E. Wieman, Phys. Rev. Lett. **101**, 040402 (2008).
- [21] S. Tojo *et al.*, Phys. Rev. A **82**, 033609 (2010).
- [22] P. Blakie, A. Bradley, M. Davis, R. Ballagh, and C. Gardiner, Advances in Physics **57**, 363 (2008).
- [23] N. P. Proukakis and B. Jackson, J. Phys. B **41**, 203002 (2008).
- [24] E. Zaremba, T. Nikuni, and A. Griffin, J. Low Temp. Phys. **116**, 277 (1999).
- [25] A. Griffin, Phys. Rev. B **53**, 9341 (1996).
- [26] D. A. W. Hutchinson, E. Zaremba, and A. Griffin, Phys. Rev. Lett. **78**, 1842 (1997).
- [27] R. J. Dodd, M. Edwards, C. W. Clark, and K. Burnett, Phys. Rev. A **57**, R32 (1998).
- [28] C. Gies, B. P. van Zyl, S. A. Morgan, and D. A. W. Hutchinson, Phys. Rev. A **69**, 023616 (2004).
- [29] M. O. C. Pires and E. J. V. de Passos, Phys. Rev. A **77**, 033606 (2008).
- [30] P. Öhberg and S. Stenholm, Phys. Rev. A **57**, 1272 (1998).
- [31] C.-H. Zhang and H. A. Fertig, Phys. Rev. A **75**, 013601 (2007).
- [32] P. Öhberg, Phys. Rev. A **61**, 013601 (1999).
- [33] D. S. Petrov, G. V. Shlyapnikov, and J. T. M. Walraven, Phys. Rev. Lett. **85**, 3745 (2000).
- [34] J.-B. Trebbia, J. Esteve, C. I. Westbrook, and I. Bouchoule, Phys. Rev. Lett. **97**, 250403 (2006).
- [35] M. Egorov *et al.*, Phys. Rev. A **87**, 053614 (2013).
- [36] R. W. Pattinson *et al.*, Phys. Rev. A **87**, 013625 (2013).
- [37] N. P. Proukakis, Phys. Rev. A **74**, 053617 (2006).
- [38] D. Gallucci, S. P. Cockburn, and N. P. Proukakis, Phys. Rev. A **86**, 013627 (2012).
- [39] K. Pilch *et al.*, Phys. Rev. A **79**, 042718 (2009).
- [40] W. Ketterle and N. J. van Druten, Phys. Rev. A **54**, 656 (1996).